POWDER DIFFRACTION

CAMBRIDGE
UNIVERSITY PRESS

Rietveld Texture Analysis from Synchrotron Diffraction Images: I. Calibration and Basic Analysis

Journal:	*Powder Diffraction*
Manuscript ID:	PD-CE-2013-0001.R2
Manuscript Type:	Crystallography Education
Date Submitted by the Author:	n/a
Complete List of Authors:	Lutterotti, Luca; University of Trento, Department of Industrial Engineering Vasin, Roman; University of California, EPS Wenk, Hans-Rudolf; University of California, EPS
Keywords:	Texture analysis, Synchrotron diffraction, Rietveld method

SCHOLARONE™
Manuscripts

For Peer Review Only

1 # Rietveld Texture Analysis from Synchrotron Diffraction Images: I.
2 # Calibration and Basic Analysis

3

4 Luca Lutterotti[1)], Roman Vasin[2,3)], Hans-Rudolf Wenk[2)*]

5

6 * corresponding author wenk@berkeley.edu
7 1) Department of Industrial Engineering, University of Trento, Italy
8 2) Department of Earth and Planetary Science, University of California, Berkeley CA 94720
9 3) Frank Laboratory of Neutron Physics, Joint Institute for Nuclear Research, Dubna, Russia

10

11 **Abstract**

12 Synchrotron X-ray diffraction images are increasingly used to characterize not only structural
13 and microstructural features of polycrystalline materials, but also crystal preferred orientation
14 distributions. Diffraction data can be analyzed quantitatively and efficiently with the Rietveld
15 method and here the detailed procedure is reported from the experiment to the calibration of the
16 2D detector and full analysis of the sample. In particular we emphasize the advantage of doing
17 the calibration inside the Rietveld least squares fitting instead of a preliminary graphical
18 calibration. Then the procedure is described to quantify crystal preferred orientations with the
19 Rietveld method implemented in software MAUD (Materials Analysis Using Diffraction). The
20 process is illustrated for a US "Nickel" coin, a 75 at.% copper 25 at.% nickel alloy with fcc
21 structure and a strong cube texture.

22

23 Key words: Diffraction images, synchrotron diffraction, Rietveld method, texture analysis

24

25

For Review Only

I. INTRODUCTION

Recently we have described a procedure to obtain quantitative texture information from time-of-flight (TOF) neutron diffraction spectra and this has been applied to several instruments such as HIPPO at the Lujan Center of Los Alamos National Laboratory (Wenk *et al*., 2010) and SKAT at the Joint Institute for Nuclear Research in Dubna, Russia (Wenk *et al*., 2012). Here we describe a similar procedure for X-ray diffraction images, particularly images collected at synchrotron radiation sources. These X-ray images need to be calibrated and transformed to diffraction patterns and a correct procedure for the calibration is important to obtain optimal results. In addition, images collected *in situ* at high pressure may show distortions due to the influence of anisotropic stress. Smaller distortions are also present in the case of residual stresses and a special procedure is necessary to separate distortions due to detector errors from effects of lattice strains. The high resolution of X-ray diffraction images also allows characterization of microstructural characteristics such as grain size and grain shape.

Emphasis is on quantitative characterization of preferred orientation patterns in polycrystalline aggregates. The orientation of crystals (or texture) has a profound influence on anisotropic physical properties, which depend on properties of single crystals and the orientation distribution. Texture has long been studied in metals and rocks (see Kocks *et al*., 2000 for details and applications) and we assume that the reader is familiar with the basic principles of texture analysis and texture representation. Texture or crystallographic preferred orientation (CPO) describes the orientation of crystallites of phases that compose a material, relative to sample coordinates, using a three-dimensional statistical orientation distribution function (ODF). Even though the computer programs used for data analysis rely on the ODF, we will only use pole figures for representation. A pole figure is a two-dimensional projection of the three-dimensional ODF and is easier to visualize. It displays the probability density of finding poles perpendicular to *hkl* lattice planes relative to the sample coordinate system. Textures are not only important for assessing deformation histories and calculation of physical properties of polycrystals, they are also essential for crystal structure refinements (e.g. Lutterotti and Bortolotti, 2005; Grässlin *et al*., 2013), quantitative phase analysis of aggregates with preferred orientations, as well as the analysis of macroscopic stress states (e.g. Lutterotti *et al*., 2004). While texture analysis is the emphasis of this presentation, we recommend the same procedure for synchrotron diffraction

For Review Only

56 image analysis of samples with random crystallite orientation, including structure analysis of
57 highly disordered materials (e.g. Battocchio *et al*., 2012).
58 Experimental methods used to obtain diffraction images are briefly described. The Rietveld
59 method implemented in the program package MAUD, which was originally developed for
60 neutron diffraction (Lutterotti *et al*., 1997), is then applied to diffraction images. Since the first
61 such application to dinosaur tendon and salmon scale (Lonardelli *et al*., 2005), procedures have
62 been refined and have become standardized. A metal coin (US "nickel") is used as an example
63 for data analysis. This sample is very straightforward to analyze; thus beginners should be able to
64 follow our procedure on their own. In the Rietveld code MAUD there are many options on how
65 to proceed to arrive at the same answer. Here we follow one (and occasionally point out other
66 possibilities) leaving it to the more experienced user to discover the full variety.
67 Readers should first consult our publication on neutron diffraction texture analysis (Wenk *et*
68 *al*., 2010) where the situation is more straightforward and where many options are described,
69 including graphic representation and texture displays. This will not be repeated here. In a
70 companion paper (Part II) we will extend the method to complex materials such as multiphase
71 shale and *in situ* deformation studies at ultrahigh pressure (Wenk *et al*., 2013). In two
72 attachments we describe step-by-step procedures for data analysis in MAUD and provide data
73 sets that can be used by readers.
74
75 **II. DIFFRACTION EXPERIMENTS**
76 In a typical synchrotron diffraction texture experiment, monochromatic radiation is used, the
77 sample is analyzed in transmission, and the diffraction image is recorded with a CCD camera or
78 an image plate detector (Figure 1). For the coin sample, high-energy (hard) X-rays with a short
79 wavelength (λ = 0.10798 Å) were used. Hard X-rays have high penetration depth and for a
80 medium absorbing material the sample dimension can be up to 2 mm in thickness without
81 significant intensity loss. The X-ray diffraction measurements were done at the BESSRC 11-ID-
82 C beamline of the Advanced Photon Source (APS) at Argonne National Laboratory. Similar
83 experiments can be done at other beamlines on different synchrotron sources (among them ALS,
84 ESRF, HASY). The specimens are typically prepared into 1-2 mm thick slabs with parallel sides
85 and mounted on a goniometer with an aluminum pin for rotation (Figure 2). The beam size is
86 about 0.5-1 mm in diameter, and the detector, in the case of our experiment, was positioned at a

For Review Only

87 distance of about 1850 mm from the sample. The angular range that is recorded depends on
88 wavelength and sample-to-detector distance.
89 Figure 3b shows a diffraction image of an American “nickel” coin, composed mainly of
90 copper, with Debye rings corresponding to reflections on *hkl* lattice planes. The azimuthal
91 variations of X-ray intensity immediately indicate lattice preferred orientation. Debye rings are
92 smooth, indicating excellent grain statistics, which is a prerequisite for a quantitative texture
93 analysis with the Rietveld method.
94 As the relative orientations of crystals and sample are crucial to texture analysis, the
95 diffraction image recorded by the detector must correspond to a view from the sample in the
96 direction of the incident beam. This is not trivial and can be verified by taking an image with an
97 object placed in front of the detector that produces an asymmetric shadow, and then viewing the
98 image to verify its correct orientation. It may be necessary to invert or rotate the image prior to
99 the data analysis.
100 A diffraction image contains reflections from many lattice *hkl* planes of many crystals, each
101 obeying Bragg’s law. In terms of pole figure coverage on a sphere, this corresponds to two small
102 circles (due to the center of symmetry imposed in a diffraction experiment, Figure 4a). A single
103 diffraction image is not very satisfactory for pole figure coverage and often is not enough for
104 quantitative texture analysis. In order to improve coverage, the sample is therefore tilted around
105 an axis perpendicular to the incident beam (Y_M-axis in Figure 4a). Generally images at different
106 omega angles (ω) are recorded and correspondingly the coverage is improved (Figure 4b).
107 Information from several images has to be combined for quantitative texture analysis. In the case
108 of the nickel coin, five images were collected at ω=-40º, -20º, 0º, 20º, 40º, providing a coverage
109 as shown in Figure 4b. To further improve coverage, the sample could be mounted in different
110 directions and corresponding images could be combined. This was not done here. During the
111 exposure, the sample can also be translated along the horizontal axis to increase the volume
112 average and grain statistics (in this case from –2 to +2 mm). The sample coordinate system is
113 defined by three axes X_M, Y_M, and Z_M and corresponding rotations χ, ω, and φ define the
114 orientation of the sample (Figure 4a).
115 The X-ray diffraction experiment has to satisfy the following conditions:
116 • The wavelength must be known to refine instrument parameters.

For Review Only

117 • The precise location of the primary X-ray beam needs to be established by using a
118 metal pin mounted on a goniometer head to assure the beam is at the center of all
119 goniometer rotations. In our case the large instrument goniometer needs to be translated
120 until the horizontal ω rotation axis is in the beam center. Generally this center position is
121 viewed through a telescope with crosshairs for mounting samples for texture analysis in
122 the correct position and the axis rotated to verify that no movements of pin tip can be
123 detected through the telescope.
124 • When measuring textures, it is imperative to know the orientation of the sample
125 relative to the diffraction instrument, and thus the directions of diffraction vectors relative
126 to the sample for all diffraction patterns. Make necessary sketches! Figure 2 shows the
127 coin as viewed from the incident beam. Be sure that sample tilts correspond to ω-
128 rotations as illustrated in Figure 1.
129 • The sample needs to be centered in the ω rotation axis to ensure the same volume
130 element and sample-detector distance at all tilt angles. Usually this is done with a small
131 goniometer head mounted on the large instrument goniometer. On it the sample can be
132 translated and rotated.
133 • The exact detector distance and detector orientation, as well as instrument peak
134 broadening parameters need to be calibrated at least once. This is done with a powder
135 standard such as cubic CeO_2 (a = 5.4116 Å, see SRM674b-NIST certificate and also
136 Yashima *et al.*, 2003) or LaB_6 (a = 4.15689 Å, see SRM660b-NIST certificate, and also
137 Chantler *et al.*, 2004) just before and/or immediately after the diffraction experiment on
138 the textured sample. With LaB_6 a higher d-range is accessible. Using the standard the
139 detector geometry and instrumental part of diffraction peak broadening are refined for the
140 calibration and then kept constant during the Rietveld analysis of the sample.
141 • You need to know detector dimensions and characteristics. As an example the
142 Perkin Elmer amorphous silicon large area detector used for the coin study at APS has
143 dimensions of 2048x2048 pixels and a pixel size of 200x200 μm.
144

For Review Only

145 **III. INSTRUMENT AND DETECTOR CALIBRATION WITH THE RIETVELD**
146 **METHOD**

147 While experiments are fast, data analysis is quite involved to advance from diffraction
148 images to quantitative orientation distributions. The Rietveld method (Rietveld, 1969) was
149 originally developed for structure analysis from neutron powder diffraction patterns and has been
150 greatly expanded since then. Currently freely available software versions that implement
151 quantitative texture analysis are the General Structure Analysis System (GSAS; Von Dreele,
152 1997; Larson and Von Dreele, 2004) and Materials Analysis Using Diffraction (MAUD;
153 Lutterotti *et al*., 1997; Lutterotti, 2010). Vogel et al. (2004) compared results for neutron
154 diffraction texture analysis by these two programs.

155 In this section we focus on image processing and calibration. Independent from the type of
156 analysis to be done, we need to measure and analyze first an appropriate standard to calibrate the
157 2D detector (distance, center, tilting and also the wavelength if it not known with accuracy) and
158 then use the calibration for the subsequent analyses with the actual samples.

159 One way to perform the detector/image calibration is with graphical routines as implemented
160 in software Fit2D (Hammersley 1998, download from
161 http://www.esrf.eu/computing/scientific/FIT2D/). In Fit2D the "calibrant" method is used for the
162 standard. After choosing a few points on an inner diffraction ring, the program will find the best
163 center (*x* and *y* detector coordinates), detector tilting errors and detector distance or wavelength,
164 by fitting the maximum intensities on a certain number of points on the Debye rings with the *d*-
165 spacings from the standard. We advise not refining both distance and wavelength as they are
166 highly correlated at low angles (high energy). Here we did not refine the wavelength. The
167 procedure of Fit2D is quite precise and accurate, but in this paper we propose a different way to
168 perform the detector calibration to resolve possible problems arising later with the analysis of the
169 actual samples, in particular:

170 - The Fit2D procedure treats the deviation of Debye rings from perfect circular shape (i.e.,
171 ovals) as due to tilting errors of the detector, excluding other causes such as
172 macroscopic mechanical strains in the sample such as for *in situ* high pressure
173 experiments. This could be corrected if the centering of the images does not change
174 between the standard and the strained sample, but this is often not the case.

For Review Only

175 - In the case of a highly textured sample or a nanocrystalline material, it is very difficult to
176 determine accurately the image center graphically using these procedures as the Debye
177 rings are more like distributed points or segments, or the lines (especially of
178 multiphase/disordered materials) are too broad for a precise localization of the maxima.
179 - In case the texture is not of interest, a common procedure is to integrate over the whole
180 Debye rings to reduce everything to only one "randomized" pattern. Eventual centering
181 errors or deviation of rings from round shape are then causing additional broadening of
182 the diffraction lines with no possibility to correct such errors later.
183 The procedure implemented in the Rietveld software MAUD (Lutterotti, 2010) relies instead
184 on a first reduction of the diffraction image into several patterns using a graphical centering with
185 no tilting errors. This pre-centering does not need to be perfect. The original image coordinates
186 are recorded for each point of each pattern. The errors in centering and tilting are subsequently
187 refined during the Rietveld refinement along with the other parameters, using a calibration
188 function that calculates each time the correct 2θ value of all data points based on the actual
189 values of such parameters.
190 The formula used for the transformation of the image coordinates into 2θ is the following:

191 $$\cot(2\theta) = \frac{D}{r\cos\delta} - \tan\delta, \qquad (1)$$

192 where

193 $$\tan\delta = \frac{-x\cos\delta_y \sin\delta_x + y\sin\delta_y}{r}, \qquad (2)$$

194 $$r = \sqrt{x^2 + y^2}, \qquad (3)$$

195 $x = x_r \cos\eta - \Delta x_c$ is the image coordinate x from the true center, (4)

196 $y = x_r \sin\eta - \Delta y_c$ is the image coordinate y from the true center, (5)

197 D is the sample-to-detector distance, δ_x is the detector tilting along x axis (rotation around y
198 axis), δ_y is the detector tilting along y axis (rotation around x axis), Δx_c is the x centering error,
199 and Δy_c is the y centering error.
200 During the reduction of patterns we save for each point the radial distance from the original
201 center and the angle η of the pattern (angular coordinate around the diffraction rings, from 0 to
202 360°, Figure 4a).

For Review Only

203 This procedure has several advantages:
204 - the calibration inside the Rietveld least squares refinement is much more effective and
205 accurate than on the image because it uses the entire peak profile and not only a
206 maximum of the circle lines;
207 - the centering can be refined also for difficult cases such as nanocrystalline sample, fiber
208 diffraction or highly textured samples;
209 - we can separate the deviation of Debye rings from round shape due to anisotropic
210 macroscopic strains from detector tilt as these two have a different dependence on 2θ;
211 - we observe generally an improved peak resolution and separation using this procedure
212 over Fit2D due to the better centering and tilting correction (especially for high
213 angle/low energy experiments).
214 The procedure is quite efficient and can be applied also to detectors in asymmetrical
215 positions and not perpendicular to the beam. In this paper we will only show the case of a
216 detector roughly perpendicular and centered with respect to the beam.
217 The procedure in MAUD always corrects the 2θ position of the experimental points rather
218 than the calculated position of the diffraction peaks. The same applies to other instrumental
219 errors like a 2θ displacement used in the traditional Bragg-Brentano geometry. The Fit2D and
220 MAUD methodologies give similar results as long as the 2θ correction is small.
221 In Table 1 we compare results of the detector calibration using the "calibrant" procedure in
222 Fit2D and by fitting directly in Maud. Two standards and wavelengths have been used. The
223 CeO_2 corresponds to the APS experiment, LaB_6 data were collected at XRD1 of the Elettra
224 synchrotron in Trieste (image plate detector). The center y coordinate in Fit2D has been
225 converted to the MAUD convention (the 0 for y is on the top-left corner and the coordinate goes
226 down; in Fit2D is lower-left corner and goes up). Also the signs of the detector tilts has been
227 reversed in Fit2D to compare with the MAUD convention. We notice considerable differences,
228 far beyond the estimated standard deviation.
229 The stack of experimental spectra can be viewed with the "Plot 2D" tab in which all
230 individual 72 patterns is displayed (Figure 5a). This image is after instrument corrections have
231 been refined and diffractions appear as straight lines. Figure 5b is the sum of individual patterns
232 ("Plot") with tick marks below showing positions of diffraction peaks. Crosses are experimental
233 data points and the line represents the Rietveld fit. Note that in not only reproduces positions and

For Review Only

234 intensities but also peak shapes. For diffraction data a square root scale for intensity is quite
235 useful, as smaller peaks are more visible.
236 The full step-by-step procedure in MAUD to calibrate the detector and instrument parameters
237 is reported in Appendix 1 and corresponding data files can be downloaded from http://PD-
238 journal.
239
240 **IV. NICKEL COIN ANALYSIS**
241 Once we have calibrated the detector and determined the instrument resolution we can
242 proceed with the analysis of the coin.
243 To perform a texture analysis we need a sufficient number of data in order to measure a
244 representative number of grains in different orientations. We need to cover the entire orientation
245 space to ensure the validity of the results. For the estimation of the microstructure we rely on
246 diffraction line broadening and for this it is critical to have a good characterization of the
247 instrumental line broadening that is obtained during the experiment with the standard. The
248 refinement strategy for the microstructural characteristics of the sample in MAUD is different
249 than in other Rietveld programs such as GSAS. There is a clear separation between the
250 instrument line broadening model and the line broadening model related with the sample. This
251 permits to refine directly only the quantities of interest concerning the sample and keep constant
252 parameters associated with the instrument.
253 The general procedure with the sample analysis is to do the integration of each image in
254 slices using the same center and parameters used for the integration of the standard image. Then
255 we use the same distance, centering and tilting errors as refined in the standard analysis. If the
256 beam centering did not change we should have a perfect calibration of the patterns (*e.g.*,
257 transformation of detector coordinates to 2θ angles). But having all the patterns around the center
258 separated in slices we can also refine centering errors if necessary. In this analysis we will refine
259 the centering for the sample, as in general it is not the same as for the standard. The center of the
260 Debye rings corresponds to the position of the diffracting volume of the sample. For the coin
261 sample it correspond to the beam position as the beam is entirely inside the sample; but the CeO_2
262 standard powder was in a capillary and thus the standard was entirely in the beam, and its
263 position inside the beam defined the centering.

For Review Only

264 The only difference with the image integration with respect to the standard is that we choose
265 a different azimuthal integration step around η (eta) angle based on the texture strength and/or
266 grain statistics. We use a 5° step to integrate along the diffraction rings (corresponding to 72
267 patterns per image). It is important to check the original diffraction image and regular intensity
268 variations around diffraction rings. The size of the integration step should be chosen sufficiently
269 small so that variations (and corresponding ODF peculiarities) are clearly distinguishable. But on
270 the other hand, intensity variations due to poor grain statistics ('spotty' diffraction images)
271 require the larger integration steps to effectively increase grain statistics. We have to determine if
272 one image is sufficient to calculate the ODF. It depends on the crystal symmetry of the
273 compound, on sample symmetry and, in principle, on the orientation distribution itself (*e.g.*,
274 when dealing with a polycrystalline phase where large parts of orientation space have
275 corresponding ODF values equal to zero, the amount of necessary measurements greatly
276 decreases, but such information is rarely available beforehand). In general it is advantageous to
277 have several images providing a wider pole figure coverage (Figure 4b versus 4a).
278 We will start the analysis using only one image ($\omega = 0°$, with the beam perpendicular to the
279 coin's face) (Figure 4a) and then add other images to improve the ODF coverage (Figure 4b). In
280 the tutorial (Appendix 2) we will show the step-by-step procedure with all images. The image
281 has been loaded as for the standard and integrated in 5° step in η to transform it into 72
282 diffraction patterns (note that in Figure 4 we show 10° increments because it is easier to view).
283 For the instrument description we import the parameters calibrated with the standard, and we
284 only refine the error in centering (2 parameters: x, y) along with the general intensity and the
285 background. We can refine the unit cell parameter of the phase (a) as both the detector distance
286 and the wavelength are kept constant.
287 After refining instrument parameters, backgrounds and lattice parameter we proceed with the
288 refinement of texture and microstructure. The strategy is similar to a normal Rietveld refinement,
289 taking into account that to fit intensities correctly we also need to refine the texture.
290 There is only one phase in this sample and it is a f.c.c. copper structure with some nickel as
291 atomic substitution. We start from a pure copper phase and substitute part of the copper with
292 nickel (25 at.% of Ni) and adjust the unit cell parameter to accommodate this change. For the
293 microstructure, we choose the default line broadening method in MAUD that correspond to the
294 simple "Delft" model (see De Keijser *et al.*, 1982 and Delhez *et al.*, 1993) and isotropic

For Review Only

295 crystallite size and microstrain for the phase. This simple model which attributes Lorentzian
296 broadening for the finite crystallite size and Gaussian broadening for the microstrain is sufficient
297 to describe the diffraction profile of the Cu-Ni phase in this sample. No anisotropic peak
298 broadening was observed.

299 For texture model we choose EWIMV (the algorithm is described in Lutterotti *et al.*, 2004)
300 that has all the features of the direct discrete WIMV method (Matthies and Vinel, 1982) but has
301 been reformulated to work within the Rietveld method. The EWIMV is able to work with
302 arbitrary pole figure grids. The value P_{hkl} on the pole figure for a certain reflection *hkl* can be
303 computed using a numerical integration (here denoted with an integral) of ODF values over the
304 proper path inside the orientation space that is considered to be discrete (divided onto quasi-
305 rectangular cells). Instead of using only the ODF values in the cells that the path is crossing, in
306 EWIMV all neighboring cells are also included, weighing their contribution by the inverse of the
307 distance of their center from the path r (a 'tube projection', Pawlik, 1986):
308

309 $$P_h = \int \frac{1}{K} \sum_{i=1}^{N} \frac{f_i}{r_i}, \quad (6)$$

310 where $K = \sum_{i=1}^{N} \frac{1}{r_i}, \quad (7)$

311

312 f_i is the ODF value in the cell i and N is the number of cells including the neighboring ones. The
313 use of such a tube projection ensures that the resulting orientation distribution will be sufficiently
314 smooth, also in the case of poor pole figure coverage. There are other texture models available in
315 MAUD. The harmonic model can be useful for weak textures, especially of phases with high
316 crystal symmetry, but it suffers from "ghost" effects due to omission of odd coefficients in the
317 harmonic expansion. For very strong textures standard functions (fibers or spheres in the
318 orientation space) can be used (this will be demonstrated in Part II for shale). Different texture
319 models have been discussed by Kocks *et al.* (2000, Chapter 3).

320 For a single diffraction image with no more than 9 reflections over the entire 2θ range
321 measured (including the partially visible reflections on the corners of the image), it is important
322 to ensure a sufficient coverage. We start with a cell size of 15° in EWIMV and no sample
323 symmetry. At the end of the refinement with MAUD we check the quality of the fit comparing

For Review Only

324 measured and calculated model patterns graphically with a 2D display (Figure 6) and evaluating
325 *R* factor values. There are different *R* factors to evaluate the quality of the refinement; some
326 apply to the Rietveld refinement of diffraction data and others to the texture calculation from
327 experimental pole density values. For both we use *Rw* which is the weighted R-factor (Table II).
328 Note that the R-factor is a single number to describe a very complex situation (as discussed by
329 Toby, 2006) and in the end the 2D display is more reliable to assess the quality of fit, including
330 texture (Figure 6). The coverage of the orientation space by data can be assessed with a function
331 that calculates the number of "hits" (number of integration paths through each cell in orientation
332 space) and values of "weights" for each cell in the orientation space (this plot can be activated
333 from inside the EWIMV options panel after at least one computation is performed).
334 In the MAUD console we can also retrieve the values for the *R* factors of the texture
335 computation and the minimum-maximum values of "hits" and "weights" for the coverage.
336 Looking at Table II, using 15° cells and only 1 image, the minimum number of hits is 42 and
337 also the weight is not too low. But as we decrease the cell size the "hits" number decreases (at
338 the same time R decreases). For 7.5° cells we have a minimum of 3 hits and less than 1E-3 for
339 the weight. Note that three hits is the limit for WIMV to resolve an orientation. By adding the
340 other 4 images collected at different ω angles we see a pronounced increase in the coverage.
341 Even in the case of 7.5° cells we have the minimum of 43 "hits". The R_w increases as now we are
342 using much more data and resolve more details of the ODF. Figure 8 compares pole figures for
343 some models. The 1 image, 10° cell case (Figure 8a) shows a remarkably similar pattern to the 5
344 image case (Figure 8b). The 5 image, 5° cell case (Figure 8c) is considerably noisier and at the
345 limit of resolution. After all, images were collected at 20° ω increments, resulting in a very
346 spotty 5° ODF coverage. For the 5 image, 10° cell case an ASCII file of the ODF was exported
347 and further processed in BEARTEX (Wenk et al. 1998). Figure 7d compares the BEARTEX plot
348 with a corresponding MAUD plot (Figure 7b).
349 From the microstructure model in MAUD we get a mean dimension of the coherently
350 scattering crystallites around 500 nm and the true grain size may be even larger. Generally, for
351 sizes larger than 200 nm diffraction patterns become almost insensitive to crystallite size.
352 The texture is a strong cube texture superposed on a weak rolling texture. In a cube texture
353 {100} is parallel to rolling direction (RD in Figure 7d), transverse direction (TD) and the
354 direction normal to the rolling plane (coin surface) in the center of the 100 pole figures. Cube is

For Review Only

355 indicative of recrystallization (*e.g.*, Schmidt and Lücke, 1979) and for a discussion of the
356 transition from rolling to cube during recrystallization see Figure 40 in Chapter 4 of Kocks *et al*.
357 (2000).
358 The full step-by-step procedure in MAUD to perform texture analysis on the coin sample is
359 summarized in Appendix 2 and corresponding data files can be downloaded from http://PD-
360 journal
361
362 **V. CONCLUSIONS**
363 Synchrotron X-rays provide a powerful method for quantitative texture analysis of materials.
364 Depending on sample size, beam size and wavelength, small (< 100 μm^3) to large volumes (>
365 200 mm^3) can be analyzed. Compared to neutron diffraction, electron backscatter diffraction or
366 pole-figure goniometry, data acquisition is fast and images display immediately qualitative
367 texture effects. 2D diffraction images are investigated with the modified Rietveld method,
368 allowing to refine microstructural parameters, phase volume fractions and texture. For simple
369 materials (in this case a coin) the refinement is straightforward and much can be done with an
370 automatic wizard in MAUD software within a few minutes.
371
372 **ACKNOWLEDGMENTS**
373 This project was supported by NSF (EAR-0836402) and DOE (DE-FG02-05ER15637). We
374 greatly appreciate access to beamline 11-ID-C at APS of Argonne National Laboratory and help
375 from Chris Benmore and Yang Ren. The tutorial was developed as part of a workshop at the
376 Advanced Light Source in fall 2012, supported by CDAC, APS (BESSRC), NSF-COMPRES,
377 ALS and STONE-LANL. We would like to thank Juan Gomez-Barreiro, Pam Kaercher and
378 Waruntorn Kanitpanyacharoen for useful comments and valuable input from the editor B. Toby
379 and three reviewers that helped us improve the manuscript.
380

For Review Only

381 **References**

382 Battocchio, F., Monteiro, P.J.M., and Wenk, H.-R. **(2012).** "Rietveld refinement of the structures
383 of 1.0 C-S-H and 1.5 C-S-H," Cement and Concrete Research **42**, 1534-1548.

384 Caglioti, G., Paoletti, A., and Ricci, F.P. (**1958**). "Choice of collimators for a crystal
385 spectrometer for neutron diffraction," Nuclear Instruments **3**, 223-228.

386 Chantler, C.T., Tran, C.Q., and Cookson, D.J. **(2004)**. "Precise measurement of the lattice
387 spacing of LaB_6 standard powder by the x-ray extended range technique using synchrotron
388 radiation," Physical Review A **69**, 042101, 1-11.

389 De Keijser Th.H., Langford J.I., Mittemeijer E.J., Vogels, A.B.P. (**1982**). "Use of the Voigt
390 function in a single-line method for the analysis of X-ray diffraction line broadening,"
391 Journal of Applied Crystallography **15**, 308-314.

392 Delhez R., de Keijser Th.H., Langford J.I., Loue□r D., Mittemeijer E.J., Sonneveld E.J. (**1993**).
393 "The Rietveld Method". Young R.A. (Ed.), (Oxford University Press). 132-166 pp.

394 Downs, R.T., and Wallace-Hall, M. (**2003**). "The American Mineralogist crystal structure
395 database," American Mineralogist **88**, 247-250.

396 Grässlin, J., McCusker, L.B., Baerlocher, C., Gozzo, F., Schmitt, B., and Lutterotti, L. (**2013**).
397 "Advances in exploiting preferred orientation in the structure analysis of polycrystalline
398 materials," Journal of Applied Crystallography **46**, 173-180.

399 Gražulis, S., Chateigner, D., Downs, R.T., Yokochi, A.F.T., Quirós, M., Lutterotti, L.,
400 Manakova, E., Butkus, J., Moeck, P., and Le Bail, A. (**2009**). "Crystallography Open
401 Database – an open access collection of crystal structures," Journal of Applied
402 Crystallography **42**, 726-729.

403 Kocks, U. F., Tomé, C. N., and Wenk, H-R. (**2000)**. "*Texture and Anisotropy: Preferred*
404 *Orientations in Polycrystals and their Effect on Materials Properties*" Second edition.
405 (Cambridge University Press, Cambridge). 677 pp.

406 Larson, A.C., and Von Dreele, R.B. (**2004**). "*General Structure Analysis System (GSAS)*". Los
407 Alamos National Laboratory Report LAUR 86-748.

408 Le Bail, A., Duroy, H., and Fourquet, J.L. (**1988**). "Ab-initio structure determination of
409 $LiSbWO_6$ by X-ray powder diffraction," Materials Research Bulletin **23**, 447-452.

For Review Only

410 Lonardelli, I., Wenk, H.-R., Lutterotti, L., and Goodwin, M. **(2005)**. "Texture analysis from
411 synchrotron diffraction images with the Rietveld method: dinosaur tendon and salmon scale,"
412 Journal of Synchrotron Radiation **12**, 354-360.

413 Lutterotti, L. (**2010**). "Total pattern fitting for the combined size-strain-stress-texture
414 determination in thin film diffraction" Nuclear Inst. and Methods in Physics Research, B **268**,
415 334-340.

416 Lutterotti, L., and Bortolotti, M. (**2005**). "Algorithms for solving crystal structure using texture,"
417 Acta Crystallographica **A61**, C158-159.

418 Lutterotti, L., Chateigner, D., Ferrari, S., and Ricote, J. (**2004**). "Texture, residual stress and
419 structural analysis of thin films using a combined X-ray analysis," Thin Solid Films **450**, 34-
420 41.

421 Lutterotti, L., Matthies, S., Wenk, H.-R., Schultz, A.S., and Richardson, J.W. (**1997**). "Combined
422 texture and structure analysis of deformed limestone from time-of-flight neutron diffraction
423 spectra," Journal of Applied Physics **81**, 594-600.

424 Lutterotti, L., and Scardi, P. (**1990**). "Simultaneous structure and size-strain refinement by the
425 Rietveld method," Journal of Applied Crystallography **23**, 246-252.

426 Matthies, S., and Wenk, H.-R **(2009)**. "Transformations for monoclinic crystal symmetry in
427 texture analysis," Journal of Applied Crystallography **42**, 564-571.

428 Matthies, S., and Vinel, G.W. (**1982**). "On the reproduction of the orientation distribution
429 function of texturized samples from reduced pole figures using the conception of a
430 conditional ghost correction," Physica Status Solidi (b) **112**, K111-114.

431 Matthies, S., Lutterotti, L., and Wenk, H-R. (**1997**). "Advances in texture analysis from
432 diffraction spectra," Journal of Applied Crystallography **30**, 31-42.

433 Matthies, S. **(2002)**. "20 years WIMV, history, experience and contemporary developments,"
434 Materials Science Forum **408-412**, 95-100.

435 Pawlik, K. **(1986)**. "Determination of the orientation distribution function from pole figures in
436 arbitrarily defined cells," Physica Status Solidi (b) **134**, 477-483.

For Review Only

437 Popa, N.C. (**1998**). "The (hkl) dependence of diffraction-line broadening caused by strain and
438 size for all Laue groups in Rietveld refinement," Journal of Applied Crystallography **31**, 176-
439 180.

440 Popa, N.C., and Balzar, D. (**2002**). "An analytical approximation for a size-broadened profile
441 given by the lognormal and gamma distributions," Journal of Applied Crystallography **35**,
442 338-346.

443 Rietveld, H.M. (**1969**). "A profile refinement method for nuclear and magnetic structures,"
444 Journal of Applied Crystallography **2**, 65-71.

445 Schmidt, U., and Lücke, K. **(1979)**. "Recrystallization textures of silver, copper and α-brasses
446 with different zinc-contents as a function of the rolling temperature," Texture of Crystalline
447 Solids **3**, 85-112.

448 SRM 660b; *Lanthanum Hexaboride Powder Line Position and Line Shape Standard for Powder*
449 *Diffraction*; National Institute of Standards and Technology; U.S. Department of Commerce:
450 Gaithersburg, MD (29 April 2010), 1-5.

451 SRM 674b; *Cerium Oxide (Quantitative Powder Diffraction Standard)*; National Institute of
452 Standards and Technology; U.S. Department of Commerce: Gaithersburg, MD (13 March
453 2012), 1-5.

454 Toby, B.H. (**2006**). "*R* factors in Rietveld analysis: How good is good enough?" Powder
455 Diffraction **21**, 67-70.

456 Vogel, S. C., Hartig, C., Lutterotti, L., Von Dreele, R. B., Wenk, H. –R., and Williams, D. J.
457 (**2004**). "Texture measurements using the new neutron diffractometer HIPPO and their
458 analysis using the Rietveld method." Powder Diffr. **19**, 65-68.

459 Von Dreele, R.B. (**1997**). "Quantitative texture analysis by Rietveld refinement," Journal of
460 Applied Crystallography **30**, 517-525.

461 Wenk, H.-R., Matthies, S., Donovan, J., and Chateigner, D. (**1998**). "BEARTEX: a Windows-
462 based program system for quantitative texture analysis," Journal of Applied Crystallography
463 **31**, 262-269.

464 Wenk, H.-R., Lutterotti, L., and Vogel, S.C. **(2010)**. "Rietveld texture analysis from TOF neutron
465 diffraction data," Powder Diffraction **25**, 283-296.

For Review Only

466 Wenk, H.-R., Vasin, R.N., Kern, H., Matthies, S., Vogel, S.C., and Ivankina, T.I. **(2012)**.
467 "Revisiting elastic anisotropy of biotite gneiss from the Outokumpu scientific drill hole based
468 on new texture measurements and texture-based velocity calculations," Tectonophysics **570-**
469 **571**, 123-134.

470 Wenk, H.-R., Kaercher, P., Kanitpanyacharoen, W., Lutterotti, L., Miyagi, L., and Vasin, R.N.
471 **(2013)**. "Rietveld texture analysis from synchrotron diffraction images: II. Complex
472 multiphase materials and diamond anvil cell experiments," Powder Diffraction (submitted).

473 Yashima, M., Ishimura, D., Yamaguchi, Y., Ohoyama, K., and Kawachi, K. (**2003**). "High-
474 temperature neutron powder diffraction study of cerium dioxide CeO_2 up to 1770 K,"
475 Chemical Physics Letters **372**, 784-787.

476

For Review Only

477 # Tables

478 Table I. Comparison results for CeO_2 and LaB_6 of the detector calibration using the "calibrant"
479 procedure in Fit2D and then fitting in MAUD or by fitting directly in MAUD the calibration
480 parameters of the detector. Parameters without standard deviations (in parentheses) have not
481 been refined in MAUD.

Standard (λ)	CeO_2 (0.10798 Å)		LaB_6 (0.7093 Å)	
Calibration	Fit2D	MAUD	Fit2D	MAUD
Center x (mm)	205.189	205.0897(3)	81.772	81.745(2)
Center y (mm)	204.751	204.7559(4)	81.674	81.6395(2)
δ_x (˚)	-0.093	-0.080(3)	0.258	0.2899(6)
δ_y (˚)	0.092	0.031(4)	-0.591	-0.6417(6)
Distance (mm)	1852.085	1850.584(2)	129.3505	129.344(3)
a (calibration)	5.4116	5.4116	4.15689	4.15689
a (refined, MAUD)	5.41312(3)	5.4116	4.15707(3)	4.15689
R_{wp} (%,MAUD)	4.14	8.4	2.13	6.91
2θ error (MAUD)	-0.00088(3)	-	-0.001(2)	-

482
483
484
485 Table II. Refinement and texture results for the coin analysis for different strategies. See text for
486 an explanation. OD_{max} is texture maximum in m.r.d.

Rietveld				EWIMV			OD Coverage			
images	R_w (%)	Parameters	Data number	Cell size	R_w (%)	OD max	Weight min	Weight max	Hits min	Hits max
1	27.2	12	50799	15˚	23.3	57.4	0.073	0.91	42	195
1	17.3	12	50799	10˚	10.9	50.0	0.014	0.34	14	99
1	14.4	12	50799	7.5˚	7.1	23.7	0.0009	0.19	3	75
5	23.1	48	255155	10˚	22.3	48.0	0.062	1.62	104	470
5	20.3	48	255155	7.5˚	18.8	35.4	0.013	0.81	43	296
5	16.9	48	255155	5˚	10.4	48.7	0.0015	0.31	10	156

487
488

For Review Only

489 # Figure Captions

490

491 Figure 1. Geometry of a synchrotron diffraction texture experiment.

492

493 Figure 2. Typical sample for a hard X-ray diffraction experiment: Nickel coin mounted on a pin.

494 Figure 3. Diffraction images with Debye rings measured at APS 11-IDC. (a) CeO_2 standard, (b)
495 Nickel coin, $\omega = 0°$. Images are before rotation in ImageJ.

496 Figure 4. Pole figure coverage with a single image (a) and with the sample rotated to different
497 positions (b). Definition of rotation angles is indicated. (c) Coverage after a 90° rotation to obtain
498 a view looking down on the coin. (10° is used for η increment).

499

500 Figure 5. Diffraction patterns for CeO_2. (a) Stack of experimental diffraction patterns after
501 refinement of detector; diffraction lines are straight (b). Fit of all 36 patterns of (a) summed
502 together using the calibration procedure inside MAUD.

503

504 Figure 6. Nickel coin. Observed (bottom) and calculated 72 diffraction patterns (top) at end of
505 refinement. $\omega = 0°$ image. "Plot2D" display. Lattice plane indices are indicated.

506

507 Figure 7. Plot of pole figures, comparing different coverages. (a) 1 image, 10° OD resolution; (b)
508 5 images, 10° OD resolution; (c) 5 images, 5° OD resolution; (d) 5 images, 10° OD resolution,
509 processed with BEARTEX. Equal area projection, upper hemisphere, Pole densities in multiples
510 of random distribution.

511

For Review Only

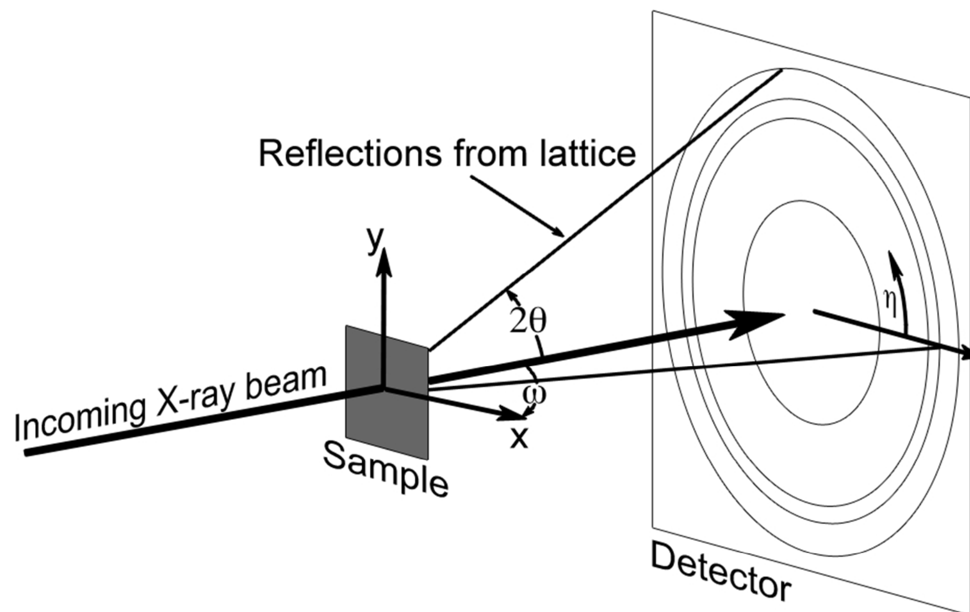

Figure 1. Geometry of a synchrotron diffraction texture experiment.

Review Only

Figure 2. Typical sample for a hard X-ray diffraction experiment: Nickel coin mounted on a pin.
17x14mm (300 x 300 DPI)

For Review Only

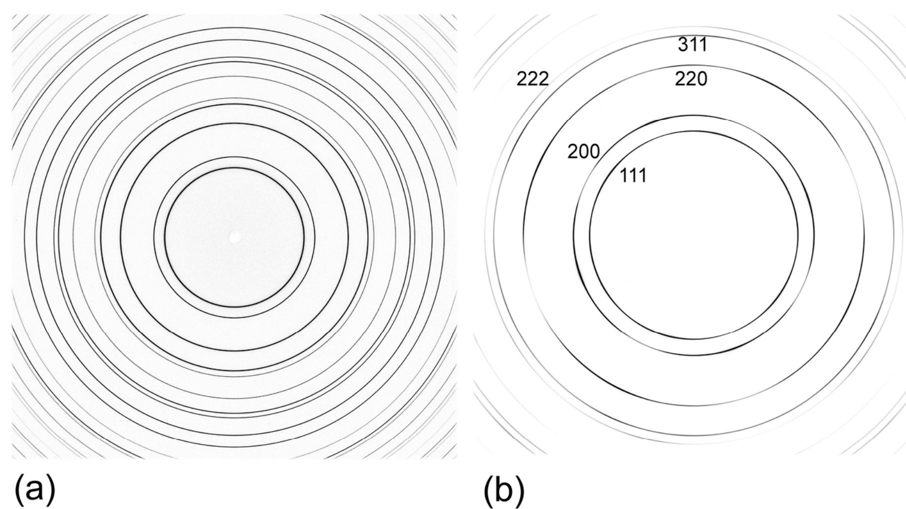

Figure 3. Diffraction images with Debye rings measured at APS 11-IDC. (a) CeO_2 standard, (b) Nickel coin, ω = 0°. Images are before rotation in ImageJ.
170x90mm (300 x 300 DPI)

For Peer Review Only

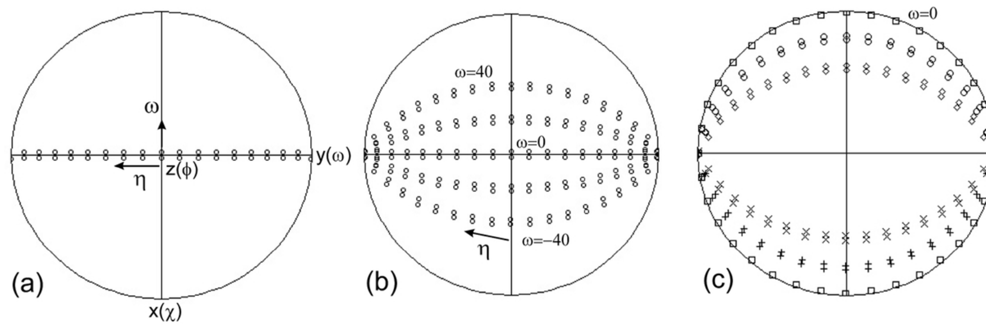

Figure 4. Pole figure coverage with a single image (a) and with the sample rotated to different positions (b). Definition of rotation angles is indicated. (c) Coverage after a 90° rotation to obtain a view looking down on the coin. (10° is used for η increment).
105x35mm (300 x 300 DPI)

For Review Only

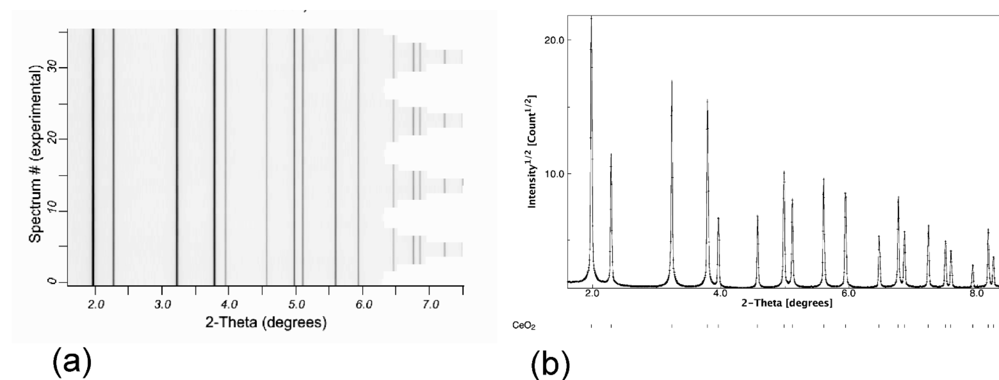

Figure 5. Diffraction patterns for CeO2. (a) Stack of experimental diffraction patterns after refinement of detector; diffraction lines are straight (b). Fit of all 36 patterns of (a) summed together using the calibration procedure inside MAUD.
333x135mm (300 x 300 DPI)

Review Only

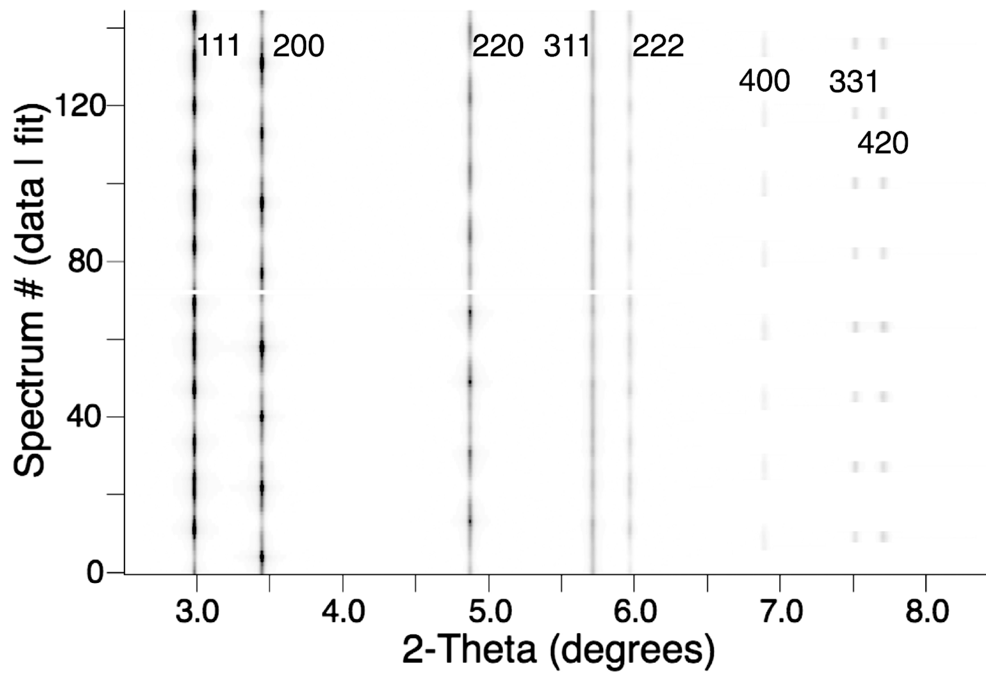

Figure 6. Nickel coin. Observed (bottom) and calculated 72 diffraction patterns (top) at end of refinement. ω = 0° image. "Plot2D" display. Lattice plane indices are indicated.
1313x887mm (72 x 72 DPI)

ew Only

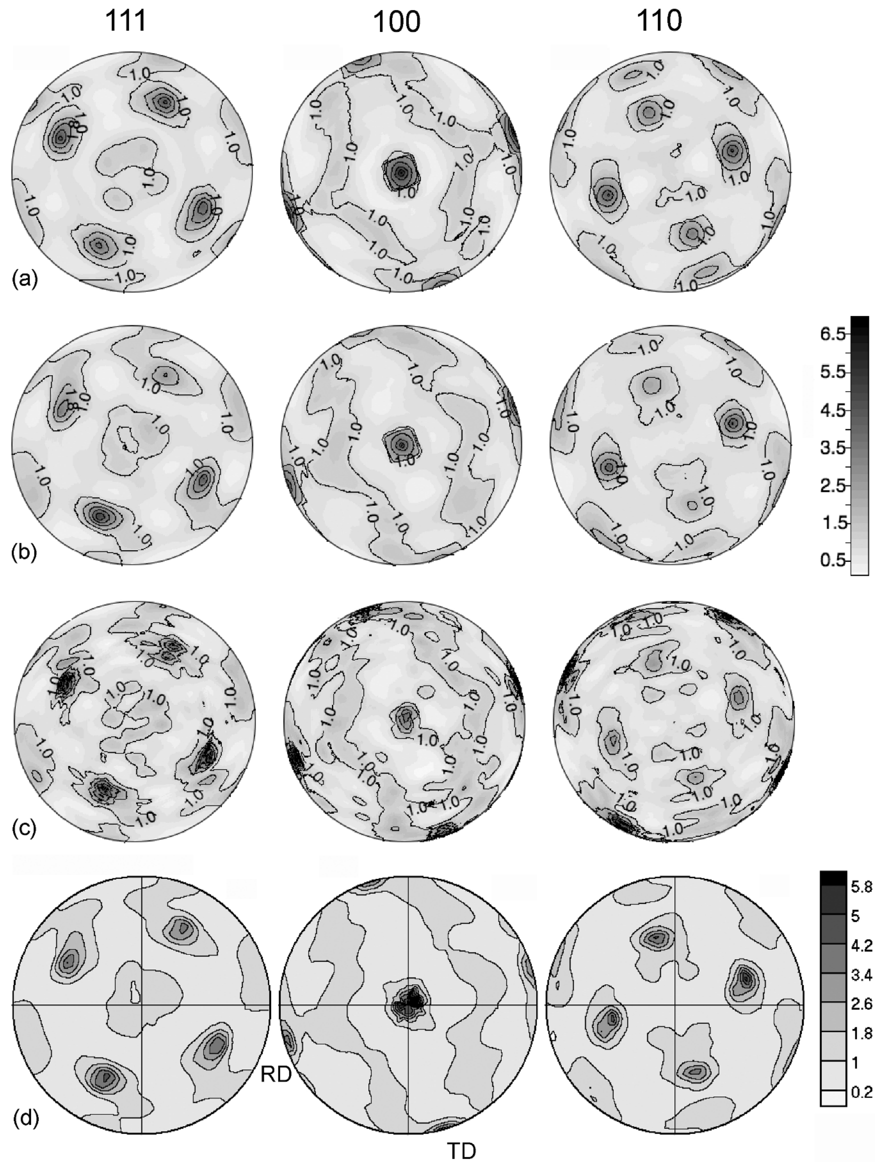

Figure 7. Plot of pole figures, comparing different coverages. (a) 1 image, 10° OD resolution; (b) 5 images, 10° OD resolution; (c) 5 images, 5° OD resolution; (d) 5 images, 10° OD resolution, processed with BEARTEX. Equal area projection, upper hemisphere, Pole densities in multiples of random distribution.
265x336mm (300 x 300 DPI)

Powder Diffraction ???, p. ??? (2014)

Rietveld Texture Analysis from Synchrotron Diffraction Images: I. Calibration and Basic Analysis

Luca Lutterotti[1)], Roman Vasin[2,3)], Hans-Rudolf Wenk[2)]
1) Department of Industrial Engineering, University of Trento, Italy
2) Department of Earth and Planetary Science, University of California, Berkeley CA 94720
3) Frank Laboratory of Neutron Physics, Joint Institute for Nuclear Research, Dubna, Russia

Figure numbers and references refer to main paper.

Download data files from the internet:

Refer to web page: http://www.ing.unitn.it/~maud/Tutorial/ImagesPowderDiffraction or http://eps.berkeley.edu/~wenk/TexturePage/MAUD.htm. The MAUD-Part-I.zip contains:

- Diffraction image for CeO_2 standard: CeO2-00010.tif
- Crystallography information file (crystal structure) for CeO_2: CeO2.cif
- Diffraction images for Nickel coin: Nickel-00182+40.tif Nickel-00182+20.tif, Nickel-00182+0.tif, Nickel-00182-20.tif, Nickel-00182-40.tif
- MAUD parameter file for Nickel coin with completed analysis (for checking): Nickel-coin.par

Appendix 1. Step-by-step procedure of image processing and instrument calibration with CeO_2 standard.

MAUD is written in Java and works with any operating system for which a Java implementation is available (Windows, Mac OS X, Linux, and Unix). It requires a large amount of memory (at least 2 or 4 GB is recommended for most cases where texture is involved). The latest version of MAUD can be downloaded from http://www.ing.unitn.it/~maud and installed into an own directory. A recent version of Java (1.6 or higher) also has to be installed (http://www.java.com). To run MAUD, use the MAUD.bat file in Windows systems, or MAUD.sh in Linux/Unix. Before running this tutorial, it may be useful to follow first one of the tutorials at http://www.ing.unitn.it/~maud/tutorial.html or check the video tutorials at: http://www.youtube.com/user/MaudRietveldProgram.

When you run MAUD for the first time, a window will open with many options and displays as shown in Figure A1-1. It has three main tabs (left side, top): “Datasets”, “Phases” and “Sample”. Most frequently used commands are present as icons in the toolbar, *e.g.*, “Disk” to save current analysis, ”Eye” to edit a selected object, “Calculator” to compute model diffraction patterns, “Hammer” to start a refinement, etc.

For Review Only

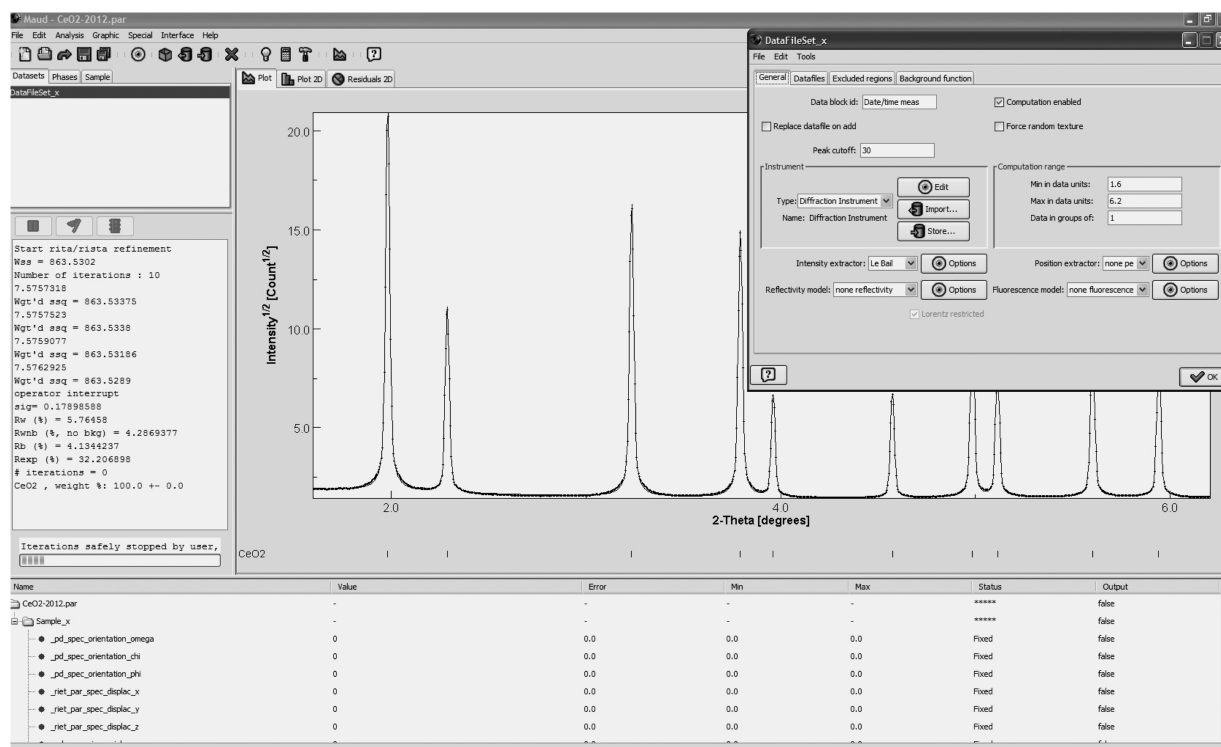

Figure A1-1. Main MAUD window on computer running Windows 7. Superposed is a window "DataFileSet" with options and settings for the selected Dataset. At the start the plot window is blank. Here data for CeO_2 standard have been entered and refined.

1. *Defining the instrument*

An instrument is defined for each dataset. Select the default dataset under "Datasets" and edit it (menu: "Edit→Edit object"), or click the "Eye" icon in the toolbar. Locate "Diffraction Instrument" in "Instrument" panel under "General" tab, and click "Edit" button. This opens the Instrument editing window (Figure A1-2).

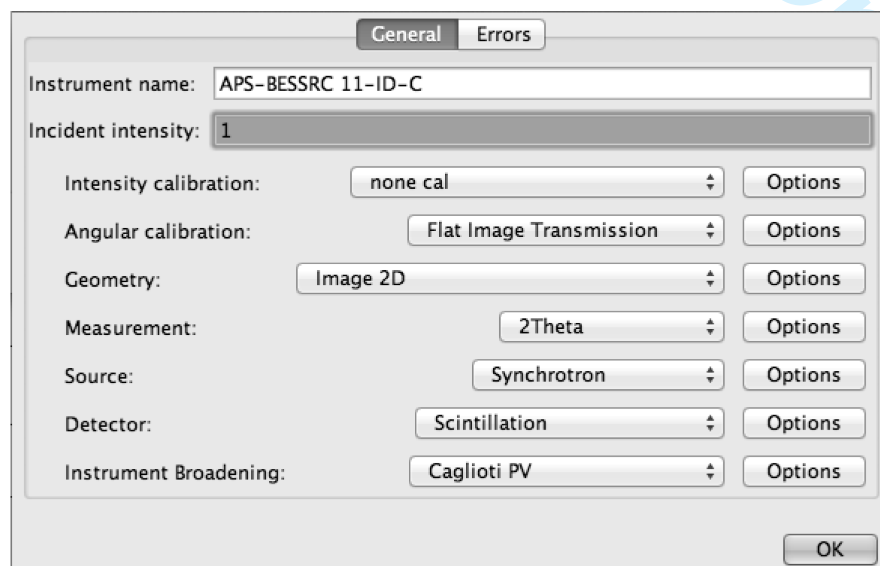

Figure A1-2. "Diffraction Instrument" window with general setup for synchrotron diffraction images.

- Rename the instrument to "APS-BESSRC 11-ID-C" so you can add it later to the instrument database and recognize it when needed.
- Adjust "Incident intensity" value to 0.001.
- Check that the option for "Intensity calibration" is "none cal".
- Choose as "Angular calibration" model: "Flat Image Transmission"; click "Options" button next to it and change the "Detector distance" to 1850 mm. The distance is needed for the conversion of image coordinates to 2θ; for now it is just an estimate and this value will be refined later. MAUD accepts data in 2θ, d-spacing or Q; everything else needs to be transformed by a calibration model.
- For "Geometry" choose "Image 2D".
- For "Measurement choose "2Theta".
- For "Source" select "Synchrotron", click "Options" and change default wavelength to 0.10798 (Å).
- In "Instrument Broadening" we should set the default parameters to be in line with synchrotron diffraction. Click "Options" button next to the "Caglioti PV" model (Caglioti *et al.*, 1958) and remove the asymmetry parameters (or set them zero). Under "HWHM" tab set all parameters to zero except for the first (the constant value, equal to W of the Caglioti formula), set it equal to 0.00025.

  Close the Instrument editing window.

2. *Entering 2D image data*

With the ImageJ plugin embedded in MAUD a .tif image file can be directly entered into MAUD and saved as .esg files, which are ASCII files containing a list of radial positions or diffraction angles and corresponding experimental intensities. If the diffraction data is in another detector format not recognized by ImageJ, it has to be converted into a regular .tif file, preserving the original intensities (e.g. for MAR detector images we advise to use the converter utility "marcvt", freely available from http://www.marresearch.com/download.html. Running marcvt in Microsoft Windows requires Cygwin (http://www.cygwin.com) with libjpeg7 and libpng12 packages. We found that using for example Fit2D for the conversion, image coordinates are inverted. Also the pixel dimension is lost in the conversion and needs to be reentered in MAUD/ImageJ before the integration).

To perform the integration in MAUD using the ImageJ library, remain in the "Datasets" window, select "Datafiles" tab (Figure A1-3). Then press the button "From images.." to start the ImageJ plugin. A small window with the typical ImageJ toolbar will appear (Figure A1-4, top right).

For Review Only

4

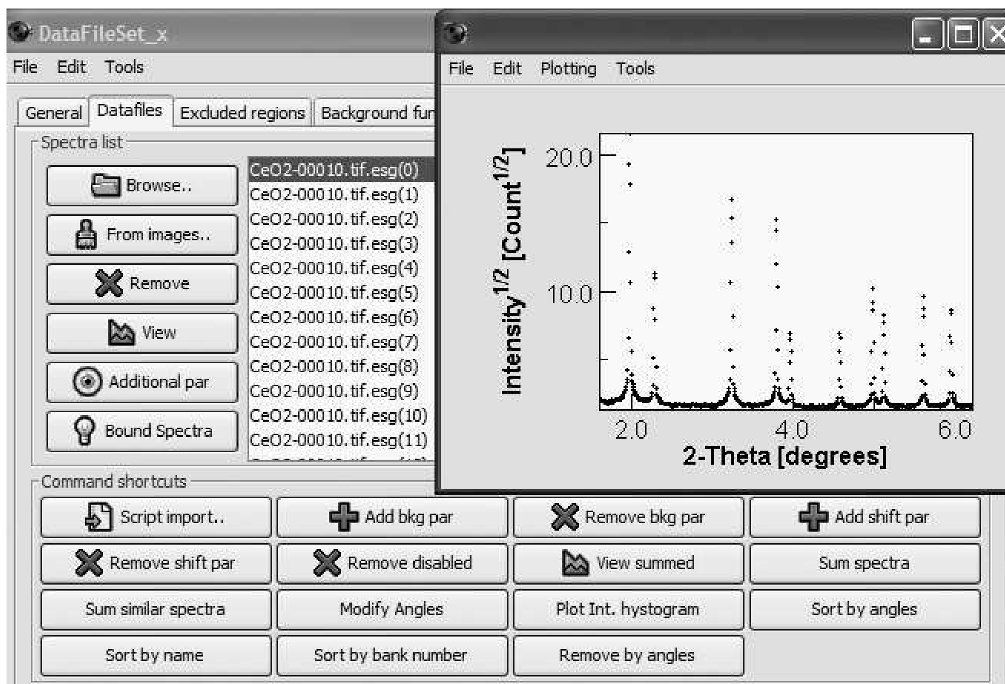

Figure A1-3. “Datafiles” in Dataset options window for CeO_2 standard, viewing one of the diffraction patterns (.esg file) in the insert. Initially there are no data in the window. In the view here they have been loaded “From images”.

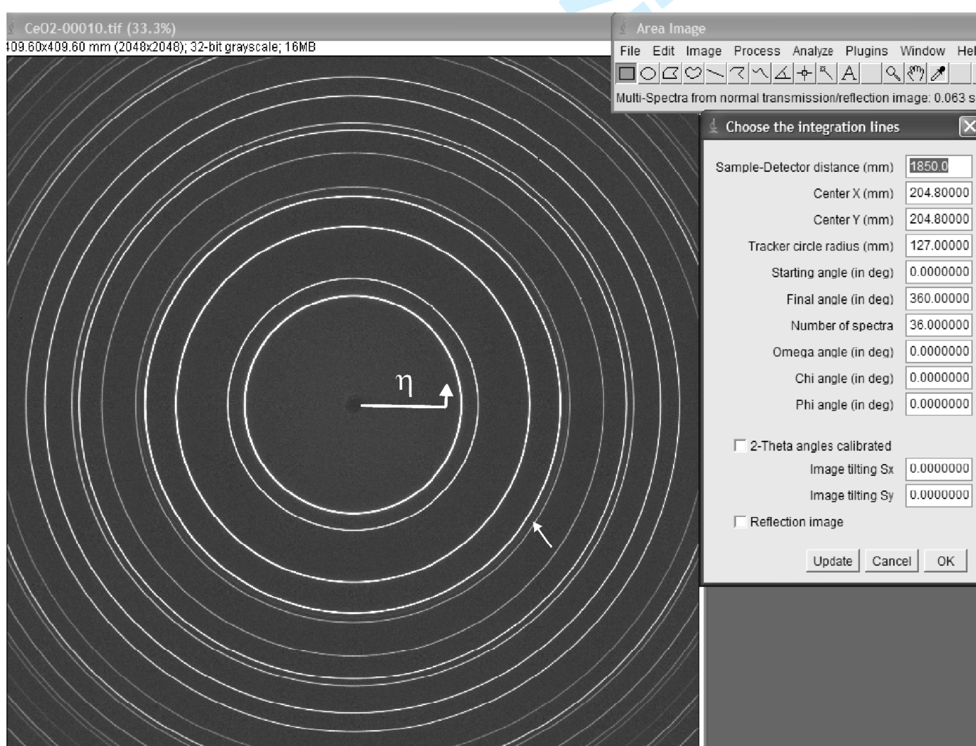

Figure A1-4. ImageJ setup for image processing to generate diffraction patterns by azimuthal integration of the 2D image. The start of η (diffraction pattern #0) is indicated. The small arrow points to the circle used for aligning the image in the center (this circle is red in the color display).

- From the ImageJ menu “File→Open…” load the image CeO2-00010.tif.
- From menu “Image→Adjust→Brightness/Contrast” use the “Auto” button as many times as you need, until you can see clearly also weaker diffraction circles or spots. Close this window.
- Select “Image→Properties”, change “Unit of length” to mm and “Pixel width” and “Pixel height” to 0.2 for the Perkin-Elmer detector (200 μm/pixel) and press “Ok”. Now on the top of the image window you should read “409.60x409.60 mm (2048x2048); 32-bit; 16MB” (Figure 11).
- Next we have to rotate the image 90° to bring the ω rotation axis for sample tilt into the origin of η to conform to the angle convention in MAUD (Figure 4a). Select “Image→Transform→Rotate 90 Degrees Left”. When using later the calibration done with this standard we have to apply the same rotation to all sample images.
- Pick the “Rectangular” selection (first button in the ImageJ toolbar) and select the ROI (Region Of Interest) to be integrated by dragging the mouse over it. If necessary, it is possible to resize it to include only diffraction rings of interest and leave out the borders where intensities may be masked or distorted.
- Now proceed to the “Plugins→Maud plugins→Multi spectra from normal transmission/reflection image”. The previous rectangular selected area will change to a red circle that now is just a tracker symbol for user’s convenience. The diffraction image appears as illustrated in Figure A1-4 (left) and next to it a “Choose the integration lines” window shows a list of parameters (Figure A1-4, right). For this sample, Sample-Detector distance is 1850 mm. If necessary adjust “Center X (mm)” and “Center Y (mm)” to bring the tracker circle (red) into the center (X = 204.85 and Y = 204.79). Adjust the tracker radius and update the plot (click “Update” not “OK” to view changes). Set the “Number of Spectra” to 72, i.e. the image will be integrated in 5° sectors. The start of the integration is indicated on Figure A1-4 (left) and the sense is counterclockwise. For each azimuthal step the integration is done for the region from η–2.5° to η+2.5°. Set Omega (ω) to 90° to bring the normal to the sample into the center of the pole figure (see section IV and Figure 4c), leave the rest to 0. Be sure that “Reflection image” and “2-Theta angles calibrated” options are unchecked (this is a transmission image and we want to use the calibration model in MAUD).
- Hit “OK” and the integration should start right away. After the integration is done, the program will ask to save the files as ASCII data. Choose the directory in which you have your data and want to perform the analysis (better not the MAUD directory). Here we give it a name CeO2-00010 (it is good practice to use the same name as the image) and the program will automatically assign “.esg” as file extension.
- Close the diffraction image and ImageJ windows and return to the MAUD dataset editing window, where the .esg files are now listed in the “Spectra list” panel. If you close the dataset window, a summation of all patterns should be visible in the plot panel of the main MAUD window (Figure A1-1).

3. *Refinement range and background*

There are no diffraction peaks at $2\theta < 1.6°$, so we restrict the refinement range in the “General” tab of the dataset editing window (Fig. A1-1, insert) by changing “Min in data units” and “Max in data units” values. Units are those of the actual diffraction data (in this case 2θ in degrees). Enter 1.6 as Min and 8 as Max.

For Review Only

Choose the background model (switch to "Background function" tab). By default a polynomial background is used in MAUD, and we use 5 parameters to approximate background by a 4th order polynomial (click "Add parameter" or "Remove parameter" buttons to change the number of parameters to 5). It is possible to assign individual backgrounds to each diffraction pattern. In the "DataFileSet" window under "Datafiles" tab, select all patterns (*i.e.*, select one and press CTRL+A on PC, or CMD+A on Mac) and in "Command shortcuts" panel add necessary number of local background parameters (click "Add bkg par" button several times; *i.e.*, three clicks will add a background function as a 2nd order polynomial to each of the selected patterns). This is not necessary here.

With this the initial setup of the diffraction instrument and the input of diffraction data is completed.

4. *Phase and initial parameters adjustment*

"Phases" tab in main MAUD window contains crystallographic and microstructural information on all the phases in the sample such as lattice parameters, space group symmetry, atomic positions, grain size, texture, etc. By default it is empty. The basic parameters can be entered as "crystallographic information files" (.cif) which can be downloaded, e.g., from databases like the ICSD (ICDD) or the COD (http://www.crystallography.net, Gražulis *et al*., 2009) or AMCSD (http://rruff.geo.arizona.edu/AMS/amcsd.php, Downs and Hall-Wallace, 2003). Some example phases are also contained in the MAUD file "structures.mdb" which comes with the installation package. To import a structure from a .cif file click the "Cylinder with arrow out" icon on the toolbar or select "Edit→Load object from CIF…" menu.

A structure model can also be built manually and with "Cylinder with arrow in" icon and saved as a .cif file for later use. To do this:

- While on "Phases" tab click the icon with the picture of a box in the toolbar (or select "Edit→Add new object" menu).
- In the "Phases" list "Phase_x" appears. It can be renamed by double clicking on it.
- Select the desired phase and "Edit" it.
- In "General" tab enter space group, and lattice parameters (for monoclinic structures first setting has to be used and for rhombohedral lattices, hexagonal setting needs to be used to comply with texture analysis conventions).
- In "Structure" tab add atomic sites to create the structure. Once a site is added, the name can be changed by double clicking the entry in the list.
- For each site, the atom type can be changed by clicking "Atom type" and selecting the appropriate atom from the Periodic table that will appear. It is possible to select the oxidation state (meaningful for x-ray scattering only) or isotope (for neutron scattering only).
- Adjust atom coordinates, site occupancies, ionization state and thermal factors if needed. Sometimes thermal factors (especially anisotropic) are loaded incorrectly from the .cif file. Check them after you import a structure.
- The created structure can be viewed in 3D by clicking the "Pointer finger" icon in the upper right corner of the structure tab window.

Here we import the provided cerium oxide structure file CeO2.cif. After it is loaded, edit the CeO2 phase. In its properties window switch to "Microstructure" tab, and click "Options" button next to "Size-Strain model: isotropic". There set the crystallite size and microstrain values to 5000 (Å) and 1.0E-5 (in means very little peak broadening from the phase).

For Review Only

After having entered all this information, pressing the "Calculator" button (or from menu "Analysis→Compute spectra") in the main page (Figure A1-1) computes diffraction patterns based on user-provided instrumental and phase parameters and compares them with experimental data. This can be viewed with the "Plot" tab above the pattern in MAUD main window which is an average over all patterns from a dataset, or with the "Plot 2D" tab in which a stack of all individual 72 patterns is displayed (experimental patterns are at bottom and model patterns are on top) (Figure 5). For diffraction data a square root scale for intensity is quite useful, as smaller peaks are more visible. This can be set or changed in "Graphic→Plot options" menu.

Next we want to adjust the scale factor (beam intensity in MAUD) as the calculated intensity data are different from experimental values. This can be done "live" by using the parameter list at the bottom of the main MAUD window (Figure A1-1). Enlarge the tree-table and scroll until you see the parameter "_pd_proc_intensity_incident" under instrument in the dataset. Make sure the column "Value" of the table is sufficiently large by dragging its border if necessary. Click on the value of the parameter you want to change (one click). Two arrows and a field to the right of the parameter appear. The text field contains the increment by which you can change the parameter by clicking on corresponding arrows. The updated plot is displayed right away. After finishing adjustments click the mouse anywhere in the tree-table (except a value) to exit from the "editing" mode. Adjust the first background parameter "_riet_par_background_pol0" in the same way.

Save your analysis as MAUD parameter file .par (e.g. name it CeO2-00010.par) in the same directory where your data are, using a menu item "File→Save analysis as…". Do not just "Save analysis" because this would overwrite the default MAUD parameter file "default.par". Your parameter file contains all information about instrument, phase and sample parameters and can be used as a starting analysis file for other images.

5. *Refinement procedure*

There are various ways to refine the parameters:

- For a manual refinement the user goes through all parameters listed in the tree-table in the bottom part of the MAUD main window and changes their status from "Fixed" to "Refined" (or "Equal to…" to set a linear dependence between different parameters). This is quite cumbersome and only applicable for experienced users. Some parameters are correlated, and some have very low impact on the calculated diffraction pattern unless other parameters values are correct, and the refinement has to proceed in a systematic order. The parameters can also be viewed by editing objects under "Datasets", "Phases" and "Sample" tabs. This is more intuitive because there the parameters are illustrated within their context, and with a right-click on the parameter you can also set it to "Refined" or "Fixed". Once you have set all the parameters you want to refine, click the "Hammer" icon in the toolbar of the main page (or select "Analysis→Refine" menu).
- Semi-automatic refinement is possible if the user selects the "Analysis→Parameters list" menu, which again displays the parameters list (click "Expand all" button below to see the entire tree-table of parameters expanded) but at the bottom there are "Commands" that allows user to change certain groups of parameters. A good start is to first "Fix all parameters" and then proceed with, *e.g.*, "Free scale pars" (general intensities and phase volume fractions are set to "Refined"), "Free backgrounds" (all parameters for backgrounds are set to "Refined"), etc. in cycles.

For Review Only

- Automatic refinement is yet another way. For this option click the “Light bulb” icon in the toolbar (or go to “Analysis→Wizard” menu) to open “Refinement wizard” and proceed with refinement from top to bottom of the list on the left side, or a complete analysis on the right side. But there is no wizard option for instrument calibration as it can not be standardized.

The refinement can be lengthy, depending on the complexities (number of patterns, number of diffraction peaks per pattern, utilization of complex texture/microstructure models, etc.). Do not change anything during the refinement! If you are reviewing some parameters in the course of the refinement, it is important to close all frames using the window close button (on all systems it is the button on the window title bar) and not with the “OK” button. The latter changes or refreshes the parameters in midst of the refinement and may cause the optimization to behave erratically.

6. *Refine scale factors and background*

We proceed with the mixture of semi-automatic and manual refinements (see step **5**). Start with “Analysis→Parameters list” and first click “Fix all parameters”, then “Free Backgrounds” and “Free scale pars”. You may leave parameters list window open to return to it later. In the MAUD main window click the “Hammer” button in the toolbar and the least squares refinement will start. Choose the number of cycles with the slider appearing at the left side of the window (usually 3-5 is sufficient). If the refinement goes well, the calculated and experimental patterns on the display should become more similar (Figure 5b, dots are experiment, line is model). Save the analysis after each successful refinement. You may want to save under different names with “Save analysis as…” in case the refinement converges into a local minimum or diverges and you need to go back a step and make manual adjustments.

7. *Refine instrument parameters*

Next we refine instrument parameters. Edit “Dataset→Diffraction Instrument” (step **1**). Under “Options” for “Flat Image Transmission” right click consecutively on values in red fields for the “Detector Distance”, “Center displacement x, and y”, “Tilting error x and y” and select “Refined” in each appearing popup menu. Close the windows and run the refinement again. This will adjust the reflection positions.

Then it is necessary to refine the instrument broadening parameters in the “Caglioti PV” model. Caglioti parameters describe instrument broadening, especially peak asymmetry, peak width and Gaussian plus Lorentzian mixing parameter (Caglioti *et al.*, 1958). These instrument peak shape parameters are essential if you want to assess peak shape effects of real samples, such as crystallite size and microstrain, or estimate dislocation density and stacking fault probability.

Caglioti parameters are very sensitive and a strict order needs to be followed. We describe the procedure for synchrotron image data where the 2θ range is limited. With the initial parameters set as suggested in step **1,** there should be no need for manual adjustments.

If you feel (or discover during the refinement) that it is still necessary, then start adjusting the first HWHM parameter – “_riet_par_caglioti_value0” – manually by using the parameter tree list in the bottom of the main window with the “live” procedure (step **4)**. After that you may adjust the second and if necessary (for large 2θ range) the third HWHM to get an approximate fit. You can view an enlarged peak by selecting an area in the plot by mouse click and dragging. Afterwards you may return to full pattern view by double clicking in the plot or right-clicking and choosing “Reset scale” from popup menu. If you need to adjust the asymmetry, then for synchrotron diffraction data we advise to start with only one parameter

For Review Only

("_riet_par_asymmetry_value0") and enter a large value (> 5000) for it if the asymmetry is small (which is usually the case for synchrotron data).

After this manual adjustment, you can proceed in the following order (3 iterations are sufficient in each of these steps; do not fix the parameters already set refined in previous steps or from beginning and be sure not to refine things like wavelength or parameters of the CeO_2 phase):

- "_riet_par_caglioti_value0", set refined and refine.
- "_riet_par_caglioti_value1", "_riet_par_gaussian_value0", "_riet_par_gaussian_value1" set refined and refine.

If you look at the plot window you can see that peak intensities are rather poorly fit. You can refine an overall thermal factor ("Edit" the phase, switch to "Structure" tab, right-click on the value of "B-factor") but this will not solve the problem completely. We can do an intensity-independent Le Bail fit for each pattern. "Edit" CeO_2, switch to "Advanced models" tab and select "Arbitrary tex" as texture model. Next fix all the scale factors or intensity-related parameters as they are not needed with the Le Bail fitting (set fixed the "_pd_processing_intensity_incident" and the "_atom_site_B_iso_or_equiv" for the Ce1 atom site). Perform another refinement cycle.

Sometimes after the refinement a message "Cholesky negative diagonal" appears in the MAUD output panel. This means the problem that MAUD was trying to solve was ill-conditioned, and some of the parameters are not refinable at the given conditions. The first of the three displayed numbers refers to the "wrong" parameter. You can view it on the MAUD output file (with .lst extension) or you may review the parameters list window and find a refined parameter with value "-1" in the "Error" column. After determining the parameter you should either adjust it manually or refrain from refining it.

8. *Saving results*

In the end, the calculated peaks should fit the experimental peaks very well, both in the "Plot" and "Plot2D" displays (Figure 5). Be sure to save the parameter file at end. To export the instrument for use in the refinement of other samples, "Edit" the current datasets and under "General" tab click "Store…" button in the "Instrument" panel to save the instrument settings as a separate file in your directory (e.g. giving it a name such as CeO2-2012.ins).

We have now refined the relevant instrument parameters with the CeO_2 standard and can apply them to other samples measured under identical conditions.

For Review Only

Appendix 2. Step-by-step procedure for texture analysis of Nickel coin.

Here we present the tutorial for the analysis of all five images but see discussion in section IV of the paper.

1. *Datasets*

Run MAUD, and create a new analysis (menu item “File→New→General analysis”). “Edit” the default dataset and under “General” tab in the “Instrument” panel click “Import…” to import the previously refined instrument file created in step Appendix 1-**8** (CeO2-2012.ins). Next, in the main MAUD window, duplicate the dataset using “Edit→Duplicate object” menu item. This will create a copy of the selected dataset including instrument parameters. Repeat this until you have 5 datasets (one for each diffraction image). Then rename the datasets (by double-clicking on its name) to, *e.g.*, “Coin-40”, “Coin-20”, etc. up to “Coin+40”.

Select the first dataset named “Coin-40” and repeat the step Appendix 1-**2** to integrate the corresponding diffraction images of the coin sample: “Nickel-00178-40.tif”. Use the same values for the image size, image rotation (90 degrees left), center X, center Y etc. that you have used for CeO_2. Only the number of patterns may be different (36 or 72 if you decide to integrate diffraction images in 10° or 5° sections), or the angles ω, χ and ϕ for the data collection. After the diffraction image integration is completed and patterns are loaded into MAUD, under “Datafiles” tab select all patterns, click “Modify Angles” button and change the ω angle (“New omega =” -40 + omega) to account for the sample tilt. For the coin it is appropriate to set the refinement range to 2.5-6.2°, as there are no diffraction peaks at lower 2θ values. In “Background function” use 5 polynomial parameters.

Repeat these operations for each of the 5 datasets, importing corresponding diffraction images and adjusting ω angles accordingly. Note that if you have several datasets then the diffraction patterns shown in all displays in the main MAUD window correspond to the currently selected dataset. To see the patterns from any other dataset you must select it in “Datasets”. When finished importing instrument and all the data, save your analysis (e.g., “File→Save analysis as…” Coin-2012.par).

2. *Phase*

Go to “Phases” tab of the MAUD main window and import the copper structure from the MAUD database (structures.mdb). Select “Copper” from the list of available phases (“Choose a Phase to add” window) and click “OK”. The structure of copper needs to be modified to take alloy composition into account. “Edit” the copper phase, go to “Structure” tab, select the Cu1 atom site in the “Site label” list and click “Duplicate”. This will make a copy of copper atom with the same coordinates, thermal factors, etc. Change the site name to Ni1 by double-clicking on it. Click the button next to “Atom type” and select Ni atom from the Periodic table appearing in a new window. Adjust “Occupancy” of Cu to 0.75 and of Ni to 0.25.

In “Advanced models” tab select the texture model. Select “E-WIMV” from the drop-down list and press the “Options” button next to it. In “E-WIMV options panel” select 10° for “ODF resolution in degrees” (see the discussion in section IV). Click “OK” in the “E-WIMV options panel” to close the window.

3. *Sample*

In the MAUD main window go to “Sample” tab and “edit” current sample. Under “Sample position” change the sample orientation angle ω to 90° degrees. This will change the orientation of the sample with respect to conventional MAUD reference coordinate system so that in pole

For Review Only

figures we look down on the Nickel coin. To check the texture coverage, first compute the model diffraction patterns (use "Analysis→Compute spectra", or "Calculator" icon), then go to the menu "Graphic→Texture plot"; select the hkl reflection for which you want to plot the texture coverage, in the "Pole figure options" panel select "Pole figure coverage" and press the "Plot" button. We set the pole figure projection plane parallel to the Nickel coin's face (as in Fig. 2) and the corresponding coverage should be similar to the one displayed in Figure 4c.

4. *Refine coin data*

In a simple case like this, the automatic "Refinement Wizard" can be used for the refinement after an approximate fit has been established manually.

Go to menu "Analysis→Wizard". Select "Texture analysis" in the panel on the right and click "Go!". This will perform the full texture analysis in 4 cycles. The first 3 cycles correspond to the refinement steps discussed in section IV (first, the refinement of backgrounds and general pattern intensities, then centering and unit cell parameters, then microstructural features); the fourth one refines the texture. Follow progress on the Plot2D display. For the first 3 cycles you will observe that the match of line positions and overall intensities between observed patterns (bottom) and calculated patterns (top) improve, but intensities in calculated patterns remain uniform. This changes dramatically in Cycle 4 (Figure 6) as texture is being refined.

With all the following parameters: 10° integration step of diffraction images, 5 diffraction images in total, refinement range in 2θ is 2.5-6.2°, 5 background parameters for each dataset, the refinement (all 4 cycles, 5 iterations per cycle) takes less than 80 seconds on a laptop with Intel Core i7 3840QM and 32 Gb of DDR3 RAM (1600 MHz, CL11) running Microsoft Windows 7 Ultimate x64 and 64-bit Java VM. If the integration of images is performed with 5° step, the computation time is increased by a factor of 2 (about 160 seconds).

5. *Checking the results*

After completion of the refinement, a first step is to check all datasets with the "Plot 2D" display to see if the intensity fit looks reasonable (Figure 6). You can also do this in a separate window by selecting "Graphic→MapPlot of selected dataset" menu. It may be also important to see how individual patterns are fitted. This is done by "Editing" a dataset of interest. Under "Datafiles" tab select one or several diffraction patterns and press "View" button. Sometimes just one or two patterns are fitted poorly, with obviously wrong peak positions, widths or intensities. You may remove such "wrong" patterns by unchecking their "Enabled" property in the same window. Repeat the refinement without them.

Check the texture pattern by selecting "Graphic→Texture plot" menu (Figure 7a-c). A new window will appear where it is possible to plot selected pole figures *hkl*, inverse pole figures, strain distributions, etc. on equal area projection. Select the pole figures to plot (check "Active" next to a set of Miller indices), ensure that "Reconstructed intensity" (i.e., pole figures calculated from ODF) and "2D map" options are selected. Then press "Plot" button. In a sub-window you have the option to change maximum and minimum values for the pole figure plot. You can plot pole figures in color or "Gray shaded". You may adjust the number of contours to draw with a slider in a bottom right part of the window, or smooth with a Gaussian filter (change "Gauss smooth width").

For Review Only

6. *Exporting texture for external programs*

Even though MAUD offers several options for plotting ODF and pole figures, it is advised to use specialized software for further texture processing. In the phase editing window under "Advanced models→E-WIMV→Options" you can export the ODF ("Export ODF formatted for Beartex"), or pole figures ("Export PFs") as ASCII files for the BEARTEX texture package. The exported ODF is always interpolated into 5°x5°x5° cells and can be converted by BEARTEX into a binary format for further processing, including smoothing, rotations, representation and physical properties calculations. Figure 7d compares a BEARTEX plot with a corresponding MAUD plot (Figure 7b).

For Review Only